

# Validation of machine learning based scenario generators

Solveig Flaig\*<sup>†</sup>, Gero Junike<sup>‡</sup>

25.10.2023

## Abstract

Machine learning methods are becoming increasingly important in the development of internal models using scenario generation. As internal models have to be validated under Solvency 2, it is imperative to understand how effective validation of these data-driven models differs from that carried out with respect to classical theory-based models. Using the specific example of market risk, we discuss the necessity of two additional validation tasks: one to check the dependencies between the risk factors used and one to detect the unwanted memorizing effect. The first task is necessary because, in this new method, the dependencies are not derived from a financial-mathematical theory but are data driven. The need for the latter task arises when the machine learning model merely repeats empirical data rather than generating new scenarios. We apply these measures to a machine learning based economic scenario generator and show that the measures lead to reasonable results for market risk modeling and can be used for validation as well as for model optimization.

**Keywords** Nearest neighbor distance, market risk modeling, Solvency 2, machine learning

**JEL classification** C14, C45, C63, G22

---

\*Corresponding author. Deutsche Rückversicherung AG, Kapitalanlage / Market risk management, Hansaallee 177, 40549 Düsseldorf, Germany. E-Mail: solveig.flaig@deutscherueck.de.

<sup>†</sup>Carl von Ossietzky Universität, Institut für Mathematik, 26111 Oldenburg, Germany.

<sup>‡</sup>Carl von Ossietzky Universität, Institut für Mathematik, 26111 Oldenburg, Germany. E-Mail: gero.junike@uol.de.

# 1 Introduction

Recently, a new class of internal models for scenario generation in the insurance and banking industry has arisen: one that uses machine learning (ML) methods. Studies that have looked at deriving a value at risk based on financial data using neural networks include Kondratyev and Schwarz (2019), Tobjörk (2021), Geller and Hainaut (2021), Fiechtner (2019) and Flaig and Junike (2022). Regulators in several countries, too, have authored papers that address considerations associated with the use of ML methods in internal models. For example, in 2019, the Nederlandsche Bank issued a paper discussing “how AI is currently already being used in finance, and what potential applications we might expect in the near future”, see van der Burgt (2019). In it, the authors state that future ML applications will “use broader and better data to develop predictive risk models”, which they anticipate will “increase the precision of risk assessment”, see van der Burgt (2019, p. 28 and 29). For their part, the German regulators, Bundesbank and BaFin, in a similar paper, BaFin (2021), assert that “the use of ML methods can help to quantify risks more accurately and enhance process quality, thereby improving financial firms’ risk management”; nonetheless, these authors also note that “the limited transparency of the model’s behavior has consequences for the [...] model validation”, see BaFin (2021, p. 7). Regulators in other countries, including France (see Dupont et al. (2020)) and Great Britain (see Jung et al. (2019)) have also issued papers on this topic.

One of the key processes for internal models in insurance companies is validation, see European Union (2009, Art. 124). BaFin (2021, p. 11), for example, notes that “supervisors are focusing on any new or much more pronounced risks that arise from ML methods. These are revealed in the data basis, validation [...], model changes and management.” Therefore, it is important to determine what additional validation measures need to be undertaken in order to prove the validity of a given model when the scenario generator is ML-based.

In response to this need, the present research, using the example of a market risk scenario generator, provides a consistent, assumption-free method for the evaluation of the dependencies between risk factors and develops a new analytic measure to detect the memorizing effect.

In studies that have examined the use of ML methods to generate financial scenarios, validation is carried out primarily by visual means or using only a few statistical parameters, as is the case in Wiese et al. (2019), Ni et al. (2020) and Wiese et al. (2020). Cont et al. (2022) propose an evaluation approach that focuses on the tail of the distribution. However, a data-driven assessment of internal model performance is desirable from two points of view: 1) to validate the model to fulfill the requirements of Solvency 2; and 2) to optimize the hyperparameters of the ML model and its architecture. In this paper we focus on both aspects.

First, in classical internal market risk models, the dependencies between the risk factors (interest rates, equities, foreign exchange) are modeled using financial mathematical tools such as correlations or copulas, see Bennemann (2011, p. 189) and Pfeifer and Ragulina (2018). However, in ML-based models, in a purely data-driven approach, the dependencies are not explicitly modeled. Therefore, an additional validation has to be performed in order to show that the dependencies generated by the model resemble the empirical dependencies in the past. For this task, we propose measures based on nearest neighbor distances, as studied by Weiss (1960); Bickel and Breiman (1983); Schilling (1986); Henze (1988); Mondal et al. (2015) and Ebner et al. (2018).

Secondly, another issue associated with generative ML models is the so-called memorizing effect, see Nagarajan et al. (2018). In this phenomenon, instead of generating new scenarios for risk management purposes, the internal model simply replicates the empirical data used in the learning process. Arora et al. (2018), for example, state that one of the most obvious pitfalls associated with GAN (generative adversarial network) training is that the GAN may simply memorize the training data. We here develop a new measure for detecting this memorizing effect as both qualitative tests and the proposed test based on the “birthday paradox”, see Arora et al. (2018), are designed for image generation and thus not suitable in general. Kim and Park (2022) also aim to detect and limit overfitting in GAN training; however, their approach requires visual inspection of the generated images for the setting of a threshold.

We make the following main contributions: we develop a measure to capture the memorizing effect and show convergence. We illustrate how to apply the nearest neighbor coincidence and the memorizing ratio measure to find an optimal GAN architecture. This extends Flaig and Junike (2022), where a GAN is used for scenario generation and this is evaluated using Wasserstein distances on marginal distributions. We enhance this evaluation here to a more broad and machine-learning adapted validation methodology.

The paper is structured as follows: In Section 2, we provide a short background on risk calculation and validation under Solvency 2. In Section 3, we introduce the two proposed validation techniques. In Section 4, we show how these techniques can be used for model validation on the example of a GAN-based economic scenario generator. Section 5 concludes.

## 2 Background: Risk calculation and validation under Solvency 2

Solvency 2 allows insurers to calculate their risk, which must be backed by capital, in two different ways. Either the standard model is used for this purpose or the insurer develops its own internal model. While in the standard model the method and the weighting factors for all risks are fixed, in the second case the insurer is free to choose the methods.

To ensure comparability of risk calculations, insurers that determine their risk using an internal model must meet certain requirements. A very important one relates to the regular validation of the internal model. According to European Union (2009, Art. 124), this “includes monitoring the performance of the internal model, reviewing the ongoing appropriateness of its specification, and testing its results against experience”.

Current internal models for market and non-life underwriting risk often use Monte-Carlo simulation techniques to derive the risk of the (sub)modules and then use correlations or copulas for aggregation, see Bennemann (2011, p. 189) and Pfeifer and Ragulina (2018). On the market risk side, the risk calculation is often based in an economic scenario generator (ESG); this approach produces realistic scenarios how the risk factors on the financial markets can behave in a certain time horizon, which is set to one year in Solvency 2, see Cadoni (2014, p. 190). ESG approaches implement financial-mathematical models for all relevant risk factors (e.g. interest rate, equity) and their dependencies. Under these scenarios, the investment and liabilities portfolio of the insurer is evaluated and the risk is given by the 0.5%-percentile of the loss in these scenarios. The models for non-life underwriting risk also simulate scenarios as to how the claims evolve and these scenarios are then used to derive the risk, see Cadoni (2014, p. 192).

An overview of various validation procedures for market risk models can be found in Herrmann and Amendinger (2017, p. 263 ff.). However, it is not appropriate to limit the validation of ML-based models to the methods used for classical financial-mathematical models. In this context, the German regulator, BaFin, warns that “Supervisory practice for ML methods can [...] be derived from the existing framework. At the same time, an outlier analysis, also supported by this consultation, is currently surveying the areas in which the supervisory inspection approach needs to be fleshed out in order to cater to the peculiarities of using ML methods.”, see BaFin (2021, p. 11). This means that the validation for an internal model can basically remain the same, but any special features of the ML-based approach must be taken into account and validated separately.

## 3 Background: Neural networks and GANs

A *neural network* is a system that is broadly inspired from the human brain. It can transpose a (one- or more-dimensional) input into a (one- or more-dimensional) output. A neural network consists of *neurons* which are arranged in *layers*. The neurons of one layer are connected to the neurons of the next layer. All starts at the left with the *input layer*, which is then followed by one or more so called *hidden layers* and ends to the right with the *output layer*, as Figure 3.1 based on Fernandez-Arjona (2021, Fig. 1) shows:

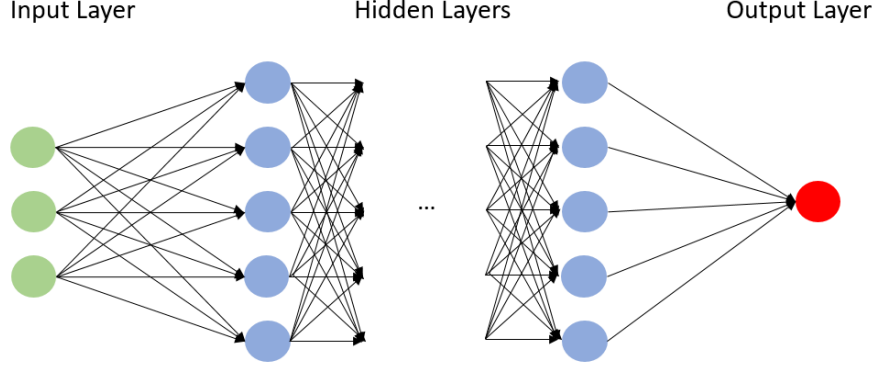


Figure 3.1: Neural network structure, based on Fernandez-Arjona (2021, Fig. 1)

All neurons transform their multi-dimensional input (which comes from either the input layer or the preceeding hidden layer) via a so called activation function into an one-dimensional output which is then transferred to all the neurons in the next layer.

A typical choice for an activation function is the rectified linear unit defined by  $g(t) = \max(t, 0)$ . Let  $x \in \mathbb{R}^n$  be the input of one neuron. Let  $w \in \mathbb{R}^{n+1}$  be some *parameters* or *weights*. The output of the neuron is defined by  $g(\sum_{i=1}^n w_i x_i + w_{n+1})$ .

The parameters in the activation function in each neuron are set randomly at the beginning. Afterwards, these parameters are optimized when giving the neural networks training data consisting of pairs of input data and the desired output so that the output of the neural network resembles the desired output given in the training data. This is repeated with new training data until some stopping point is reached. The stopping point is determined by the target funtion of the neural network.

A *GAN*, see Goodfellow et al. (2014), is a system of two neural networks (called *discriminator* and *generator*) that are cleverly interconnected to produce data that is similar to the input data, in the sense that the output data has the same distribution as the input data. For the training of the GAN, both neural networks are trained in turns in each training iteration until the generator successfully produces data that resembles the input data. In neural networks and especially in GANs, a lot of architectural and hyperparameter choices have to be made, e.g., the number of layers in each neural network, the number of neurons per layer, the activation and loss functions, etc. However, as GANs are difficult to train, see Goodfellow (2016, p. 17), the model architecture and the hyperparameters have to be chosen carefully.

We recall from Flaig and Junike (2022) a formal definition of a GAN, see also Goodfellow (2016) and Wiese et al. (2020):

Let  $(\Omega, \mathcal{F}, \mathbb{P})$  be a probability space and  $N_X, N_Z \in \mathbb{N}$ . Let  $X$  and  $Z$  be  $\mathbb{R}^{N_X}$ - and  $\mathbb{R}^{N_Z}$ -valued random variables, respectively.  $Z$  represents the latent random noise variable, and  $X$  represents the targeted random variable.  $(\mathbb{R}^{N_Z}, \mathcal{B}(\mathbb{R}^{N_Z}))$  is called the *latent space*. Usually,  $N_Z > N_X$  is chosen; see Goodfellow (2016, p. 18). We define a generator as follows:

**Definition 1.** Let  $G_{\theta_G} : \mathbb{R}^{N_Z} \rightarrow \mathbb{R}^{N_X}$  be a neural network with parameter space  $\Theta_G$  and  $\theta_G \in \Theta_G$ . The random variable  $\tilde{X} = G_{\theta_G}(Z)$  is called the *generated random variable*. The network  $G_{\theta_G}$  is called the *generator*.

The goal is to train the generator network, such that the generated random variable  $\tilde{X}$  has the same distribution as target variable  $X$ . The variable  $X$  represents the empirical data and  $\tilde{X}$  represents generated data. To train the generator, we need another neural network called discriminator and formally defined by:

**Definition 2.** A neural network with  $D_{\theta_D} : \mathbb{R}^{N_X} \rightarrow [0, 1]$  with parameter space  $\Theta_D$  and  $\theta_D \in \Theta_D$  is called a *discriminator*.

Given these two neural networks, we can now define a GAN as in Goodfellow (2016, Chapter 3):

**Definition 3.** A *GAN (generative adversarial network)* is a network consisting of a discriminator  $D_{\theta_D}$  and a generator  $G_{\theta_G}$ . The parameters  $\theta_D \in \Theta_D$  and  $\theta_G \in \Theta_G$  of both networks are trained to optimize the value function

$$V(G_{\theta_G}, D_{\theta_D}) = \mathbf{E}[\log(D_{\theta_D}(X))] + \mathbf{E}[\log(1 - D_{\theta_D}(G_{\theta_G}(Z)))]$$

with  $X$  the targeted random variable and  $Z$  the latent random noise variable.

Figure 3.2 shows the structure of a GAN based on Chollet (2018, Chapter 8.5).

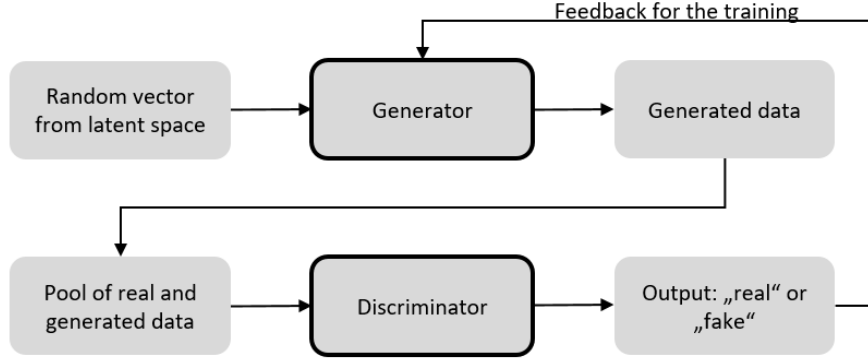


Figure 3.2: Neural network structure, in accordance with Chollet (2018, Chapter 8.5)

$Z$  can be sampled from the latent space with a any chosen distribution, however, one usually uses normal distribution for  $Z$ , see Chollet (2018, Chapter 8.5.2). The value function  $V$  has been defined in Goodfellow (2016). The optimization (the *GAN objective*) is given by

$$\min_{\theta_G \in \Theta_G} \max_{\theta_D \in \Theta_D} V(G_{\theta_G}, D_{\theta_D}).$$

That means that the discriminator is optimized to distinguish real samples from generated samples whereas the generator tries to ‘fool’ the discriminator by generating such good samples that the discriminator is not able to distinguish them from real ones. A detailed derivation of the optimization of the objective and the modifications that can be used in GAN training are found in Goodfellow (2016, p. 22) and Wiese et al. (2020, p. 9).

## 4 Validation techniques for machine learning based scenario generators

GANs can be used to generate financial scenarios, see Flaig and Junike (2022), Ni et al. (2020) and Wiese et al. (2020). In these papers, validation doesn’t take into account the specialties of machine learning, but is carried out primarily by visual means or using only a few statistical parameters, e.g. Wasserstein metric.

During the normal validation cycle for scenario generation in internal models, insurers already test many statistical properties of a scenario generator. Stability and sensitivities are also part of validation, see Herrmann and Amendinger (2017). However, with an ML-based approach, there are additional validation requirements: since the interdependencies of the risk factors are not derived from a financial mathematical model, they have to be validated separately. Furthermore, it must be checked whether the memorizing effect occurs, i.e. whether pure resampling takes place.

As Meehan et al. (2020, p. 1) states, “any method that can assess these generative models must be based only on samples produced by them”. In this research, we employ a purely data-driven evaluation approach because one of the main advantages of using ML for scenario generation is that no further (financial-mathematical) assumptions on e.g. distributions are necessary, and therefore we do not want

to use assumptions in the evaluation. Such methods are generally referred to as *model agnostic*, see e.g., Borji (2019, p. 4). Furthermore, we want to take measures that are easily interpretable so they can also be used for validation purposes in Solvency 2. Therefore, we split the recommended validation techniques into two categories:

- (1) the alignment of the dependencies between empiric and generated data
- (2) the memorizing effect.

Measures for these two categories are discussed in Subsections 4.1 and 4.2. The methods can be used not only for validation but also for hyperparameter optimization of the ML models. If one is especially interested in the tails of the distribution, one can either additionally validate the resulting risk scenarios using the quantitative measures based on value-at-risk and expected shortfall, as proposed in Cont et al. (2022, p. 21), or use benchmarking as in Flaig and Junike (2022, Chapter 3).

For the mathematical discussion in the remainder of this section, we use the following notations:

Let  $(\Omega, \mathcal{F}, P)$  be a probability space and  $d \in \mathbb{N}$  the number of risk factors that we model.  $E : \Omega \rightarrow \mathbb{R}^d$  denotes a random vector describing the empirical data. The data generated by a ML model is described by the random vector  $G : \Omega \rightarrow \mathbb{R}^d$ . Let  $m \in \mathbb{N}$  and let  $E_j$ , and  $G_j$ ,  $j = 1, \dots, m$ , be independent copies of the random vector  $E$  and  $G$  respectively. Let  $\mathbb{E}(\omega) = \{E_1(\omega), \dots, E_m(\omega)\}$  and  $\mathbb{G}(\omega) = \{G_1(\omega), \dots, G_m(\omega)\}$  for  $\omega \in \Omega$ . The target of the ML model is that the generated data  $G$  should follow the same (but unknown) distribution as the empirical data  $E$ . We denote the distribution functions of  $E$  and  $G$  by  $F_E$  and  $F_G$  and the corresponding density functions by  $f_E$  and  $f_G$ , respectively.

#### 4.1 *Measure for the alignment of the dependencies between empirical and generated data: Nearest neighbor coincidences*

The test on the alignment of the dependencies of the empirical and generated data can be reformulated as a multivariate two-sample test where we want to measure the equality of two multivariate distributions based on two sets of independent observations. For this purpose, we choose to use the *nearest neighbor coincidence measure* as defined by Schilling (1986) and as further developed by Mondal et al. (2015). This measure serves our purpose as it is easily interpretable: if the dependencies between the empirical data are correctly captured in the generic data set, then half of the nearest neighbors for all data points from each set should belong to the empirical and half to the generated data set.

Another option that we tested was the *number of statistically different bins* from Richardson and Weiss (2018), but this measure showed instabilities in our experiments. Therefore, we stick to the nearest neighbor coincidence measure. Other possibilities for detecting the alignment include e.g., maximum mean discrepancy, average log-likelihood and F1-score, see Borji (2019), but all of these methods require further assumptions and are therefore not model agnostic.

The nearest neighbor coincidence itself is defined as follows. The indicator function  $\mathbf{1}_{E_i}(l)$  takes the value 1 if the  $l$ -nearest neighbor (measured in euclidean distance) of data point  $E_i$  out of data set  $\mathbb{E} \cup \mathbb{G}$  stems from data set  $\mathbb{E}$  and zero otherwise. The indicator function  $\mathbf{1}_{G_j}(l)$  is defined similarly. Let  $k \in \mathbb{N}$ . As in Mondal et al. (2015, Chapter 2), we define by

$$T_{1,k} = \frac{1}{mk} \sum_{i=1}^m \sum_{l=1}^k \mathbf{1}_{E_i}(l)$$

the proportion of neighbors of  $E_i$  that come from  $\mathbb{E}$  and by

$$T_{2,k} = \frac{1}{mk} \sum_{i=1}^m \sum_{l=1}^k \mathbf{1}_{G_i}(l)$$

the proportion of neighbors of  $G_i$  that come from  $\mathbb{G}$ . A statistic “nearest neighbor coincidence”  $nnc_{k,m}$  is defined by

$$nnc_{k,m} := T_{NN1,k} = \frac{1}{2} \left| T_{1,k} - \mathbf{E}[T_{1,k}] \right| + \frac{1}{2} \left| T_{2,k} - \mathbf{E}[T_{2,k}] \right|.$$

Mondal et al. (2015) prove that the expectations of  $T_{1,k}$  and  $T_{2,k}$  satisfy

$$\mathbf{E}[T_{1,k}] = \mathbf{E}[T_{2,k}] = \frac{m-1}{2m-1} \rightarrow \frac{1}{2}, \quad m \rightarrow \infty$$

and that  $T_{NN1,k}$  converges to 0 in probability as  $m \rightarrow \infty$  if  $E_1, \dots, E_m, G_1, \dots, G_m$  are independent and identically distributed and have continuous densities.

## 4.2 Measure for the detection of the memorizing effect: Memorizing ratio

The nearest neighbor coincidence statistic will lead to optimal scores if the generated data points exactly match the empirical ones, i.e.,  $\mathbb{E} = \mathbb{G}$ . From a risk management perspective, this is not the optimal result because we want to create new scenarios that could happen rather than memorizing scenarios that have actually taken place, see Chen et al. (2018, p. 2). Bai et al. (2021, p. 1) emphasize that “unintentional memorization is a serious and common issue in popular generative models”. Therefore, we need to identify a measure to detect whether the generated data points really differ from the empirical ones and to ensure that the model is not simply memorizing the data points (“overfitting”).

Literature on tests for memorizing in GANs is sparse. One test to detect memorizing in generative models that we do find in literature is the birthday paradox test, see Borji (2019) and Arora et al. (2018). This test, however, is based on the visual identification of duplicates for pictures and therefore cannot be utilized in our context.

Another test is presented in Xu et al. (2018, p. 8): One holds out a part of the training data as a validation set. Then, some similarity measure (e.g., Wasserstein distance, maximum mean discrepancy (MMD), 1-NN two sample test) is calculated both between generated data and the training data as well as between generated data and the validation set. One can conclude that memorizing is taking place if these two values differ significantly. However, this requires holding out some data, which means that the amount of training data is reduced. This is unfavorable in applications in which training data is sparse. Meehan et al. (2020) also uses a hold out validation data set, but modifies this test by defining subspaces in which the measures are calculated.

Bai et al. (2021) introduce a measure called memorization penalty to detect whether the cosine similarity between generated and training data is below a certain threshold. However, this threshold is chosen based on over 11,000 generative models and is chosen in such a way as to distinguish two groups of submissions (memorized vs. non-memorized). This measure is useful for classifying various models if many are involved, but does not fit our purpose for validation of a single model.

Webster et al. (2019) also studies the issue of overfitting in GAN models and come to the conclusion that a separate measure is needed to detect memorizing in GANs as this is not detected when using only standard statistics or two-sample tests. In Webster et al. (2019, Chapter 3.4), a measure called median recovery error is suggested, but this measure is designed for image generating GANs and can therefore not be applied here.

As we found no appropriate measure in the literature, we designed our own. In a multi-dimensional space, it is highly unlikely for generated and empirical data points to match exactly, so we classify a empirical data point  $E_i$  as being memorized if a generated data point lies in “an unusual small neighborhood” around this empirical data point. We here define an “unusual small neighborhood” as a fraction  $0 < \rho \leq 1$  of the 1-nearest neighbor distance of an empirical data point  $E_i$  to the next empirical data point. If a lot of empirical data points are closely surrounded by generated data points, then the generated data set does not significantly differ from the empirical one. The memorizing ratio, defined next, describes the proportion of empirical data points for which the unwanted memorizing effect occurs.

**Definition 4.** Let  $\omega \in \Omega$ ,  $\rho \in (0, 1]$ . The realization  $E_i(\omega)$  is called *being memorized* if there is a  $k \in \{1, \dots, m\}$  such that

$$|G_k(\omega) - E_i(\omega)| \leq \rho \min_{\substack{j=1, \dots, m \\ i \neq j}} |E_j(\omega) - E_i(\omega)|.$$

with  $|\dots|$  being the Euclidean distance in  $\mathbb{R}^d$ .

This definition is now extended to the whole data set to define the proportion of empirical data points that are memorized:

**Definition 5.** Let  $\rho \in (0, 1]$  and  $m \in \mathbb{N}$ . The *memorizing ratio*  $mr_{\rho, m}$  is defined as:

$$mr_{\rho, m} = \frac{1}{m} \sum_{i=1}^m \mathbf{1}_{[0, \rho R_{E_i}^1)} \left( \min_{j=1, \dots, m} |G_j - E_i| \right) \quad (4.1)$$

where  $R_{E_i}^1$  is the distance between  $E_i$  and its 1-nearest neighbor out of  $\mathbb{E}$ , i.e.,

$$R_{E_i}^1 := \min_{i \neq j} |E_i - E_j|, \quad i = 1, \dots, m.$$

The benefit of the memorizing ratio can be visualized in Figure 4.1.

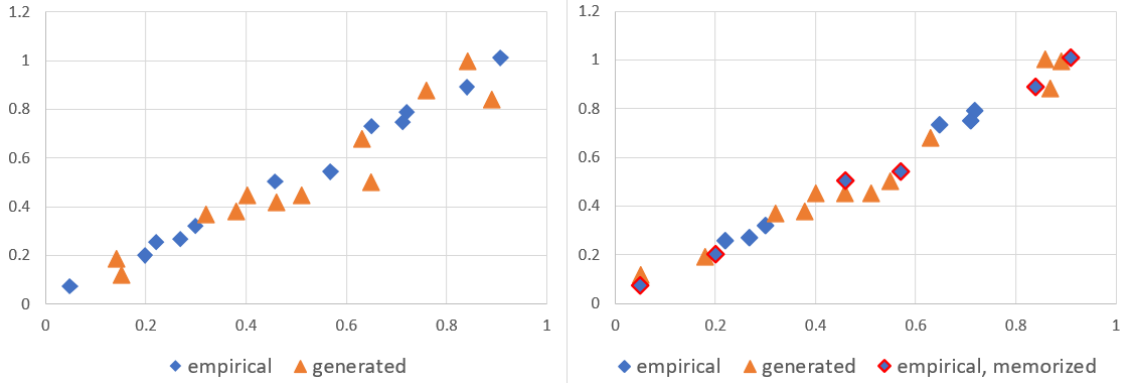


Figure 4.1: Example for the benefit of the memorizing ratio; on the left:  $nnc_{3,12} = 0$ ,  $mr_{0.5,12} = 0$ ; on the right:  $nnc_{3,12} = 0$ ,  $mr_{0.5,12} = 0.5$ .

Both graphs show in blue the same 12 empirical data points. In orange, 12 different generated data points are shown. In both experiments, the nearest neighbor coincidence for  $k = 3$  is at its optimal value,  $nnc_{3,12} = 0$ . However, one can clearly see that on the left-hand side the variability of the generated data points is higher than on the right. The memorizing ratio here can be used to penalize the behavior where the generated data points are very close to the empirical ones: on the left side, the memorizing ratio with  $\rho = 0.5$  is zero ( $mr_{0.5,12} = 0$ ), whereas on the right side, 50% of the empirical data points are categorized as memorized ( $mr_{0.5,12} = 0.5$ ). The memorized data points are framed in red.

For risk management purposes, it is important that new data points are created rather than existing ones memorized. Therefore, the memorizing ratio here supports this objective.

Next, we show that the memorizing ratio converges in mean square.

**Theorem 6.** *If the random variables  $E_1, \dots, E_m, G_1, \dots, G_m$  are independent and identically distributed and  $E_1$  has a piecewise continuous and bounded probability density function  $f$ , the memorizing ratio  $mr_{\rho, m}$  converges in mean square to  $\frac{\rho^d}{\rho^d + 1}$  for  $m \rightarrow \infty$ .*

*Proof.* The proof is devoted to the Appendix A.

To check for the convergence stated in theorem 6 empirically, we conducted a numerical experiment for  $\rho \in \{0.1, 0.3, 0.5, 0.7, 0.9\}$  in two dimensions and with different distributions (standard normal, exponential with mean 1, t-distribution with 1 degree of freedom, Cauchy with scale and location equal to 1, Pareto with scale and shape equal to 1). We randomly sample two data sets from the same distribution with two different numbers of points,  $m = 500$  and  $m = 5000$ . Then, we calculate the memorizing ratio between these two samples. We repeat this procedure 100 times and compute the average of the memorizing ratio. The results are shown in Table 1.  $\square$



$d$	$\rho$	normal	exponential	Student's t	Cauchy	Pareto	theoretical
2	0.1	0.009/0.010	0.010/0.010	0.011/0.010	0.012/0.010	0.012/0.011	0.010
2	0.3	0.082/0.083	0.084/0.083	0.084/0.083	0.090/0.085	0.089/0.085	0.083
2	0.5	0.200/0.200	0.201/0.201	0.198/0.199	0.207/0.202	0.204/0.203	0.200
2	0.7	0.3289/0.329	0.330/0.330	0.325/0.328	0.333/0.330	0.332/0.330	0.329
2	0.9	0.452/0.448	0.444/0.449	0.442/0.447	0.447/0.447	0.446/0.447	0.448

Table 1: Expectation of the memorizing ratio for  $n = 100$  simulations, with  $m = 500$  (first number) and  $m = 5000$  (second number) and different values of  $\rho$  for the following distributions: standard normal, exponential with mean 1, t-distribution with with 1 degree of freedom, Cauchy with scale and location equal to 1, Pareto with scale and shape equal to 1.

As one can see, the empirical values and the theoretical values match quite closely, even for more exotic distributions. Although the values of the memorizing ratio for  $m = 500$  are already quite close, the values for  $m = 5000$  are closer to the theoretical value, thus showing the convergence stated in theorem 6 empirically.

## 5 Application of the measures to a GAN-based ESG

To show how the nearest neighbor coincidence and the memorizing ratio measures can be used for validation in practice, we apply them to the GAN-based ESG as introduced in Flaig and Junike (2022). In that paper, the scenario generation for market risk simulation utilizes a generative adversarial network, called GAN. In this context, the input data consists of the rolling annual returns of 46 different financial risk factors (e.g. stock prices, interest rates, fx exchange rates) over a time period of almost 18 years, leading to 4330 training data sets in 46 dimensions.

Flaig and Junike (2022) use 46-dimensional financial data to generate scenarios and validate this using Wasserstein distance. In this paper, we want to validate the GAN architecture used in that paper (with e.g., four layers in each network) utilising nearest neighbor coincidence and memorizing ratio.

For the remainder of this article, we use  $m = 100$  data points for the evaluation to ensure computational feasibility. As in Mondal et al. (2015), we set the parameter for the nearest neighbor coincidence  $k = 3$  and write  $nnc$  instead of  $nnc_{3,100}$ . For the memorizing ratio, we use  $\rho = 0.5$  and write  $mr$  instead of  $mr_{0.5,100}$ .

In Figure 5.1, we see the contrasting behavior of the two measures over the training iterations. The  $nnc$  starts higher and is declining. This implies that at the beginning of the training the generated data does not resemble the empirical data, but in the course of the training an increasingly accurate replication of the empirical distribution is achieved. The  $mr$ , however, starts with 0 and is increasing over the iterations. This indicates that more and more scenarios are generated that were already contained in the training data in this or in a very similar way. Each insurance company must then find the balance between these opposing measures, as a memorizing ratio of 0.1 means that only 90% of the scenarios are newly generated.

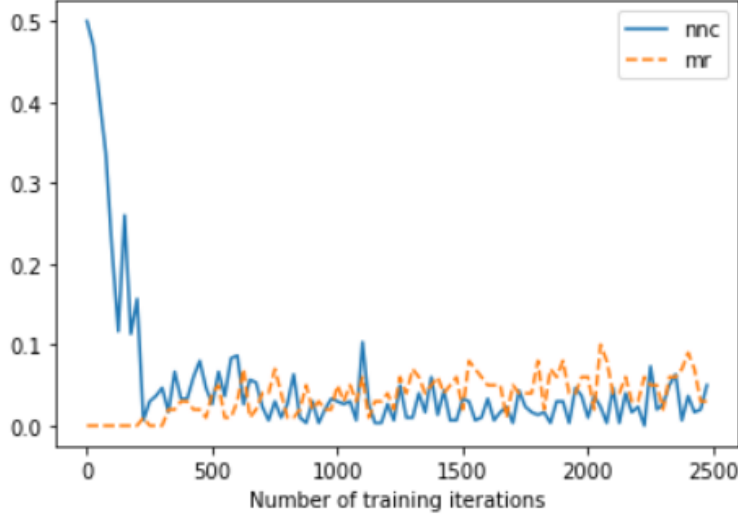


Figure 5.1: Development of the chosen validation measures  $nnc$  and  $mr$  for the GAN-based ESG

To provide a closer look at the memorizing ratio, we analyzed the distances between a generated point and its nearest empirical data point. For 100 generated data points, we evaluated the Euclidean distances in 46 dimensions to the respective next empirical data point at two different training iterations: 650 and 1300 with  $mr$  being 1% and 8%.

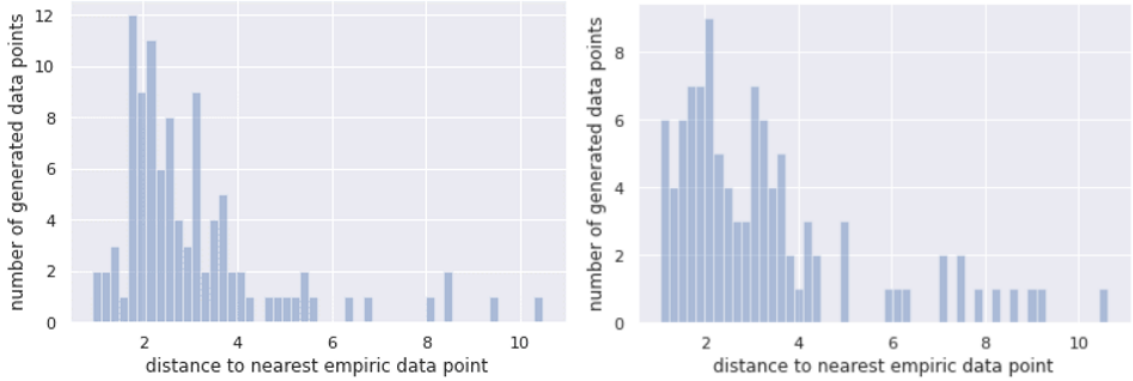


Figure 5.2: Comparison of two histograms for the distances between a generated point and its nearest empirical data point; left: 650 training iterations,  $mr = 1\%$ ; right: 1300 training iterations,  $mr = 8\%$

Figure 5.2 shows that if the memorizing ratio is lower (left), the number of generated data points that are very close to an empirical data point (e.g., when looking at distances between 0 and 1 in the figures above) is, as expected, significantly lower than for a higher value of the memorizing ratio (right). This means that in a real setting the memorizing ratio is able to detect when generated data points are very close to the empirical ones.

To get some benchmark on the performance of the GAN-based model using the measures  $nnc$  and  $mr$ , we implement a dummy model for data generation. This dummy model simply generates new data by multiplying each value of the empirical data of each of the 46 risk factors by some random number. Each random number is normally distributed with mean 1 and a fixed standard deviation  $\sigma$ . For the Figure 5.3, we vary  $\sigma > 0$  between 0.001 and 0.2 and calculate  $nnc$  and  $mr$ .

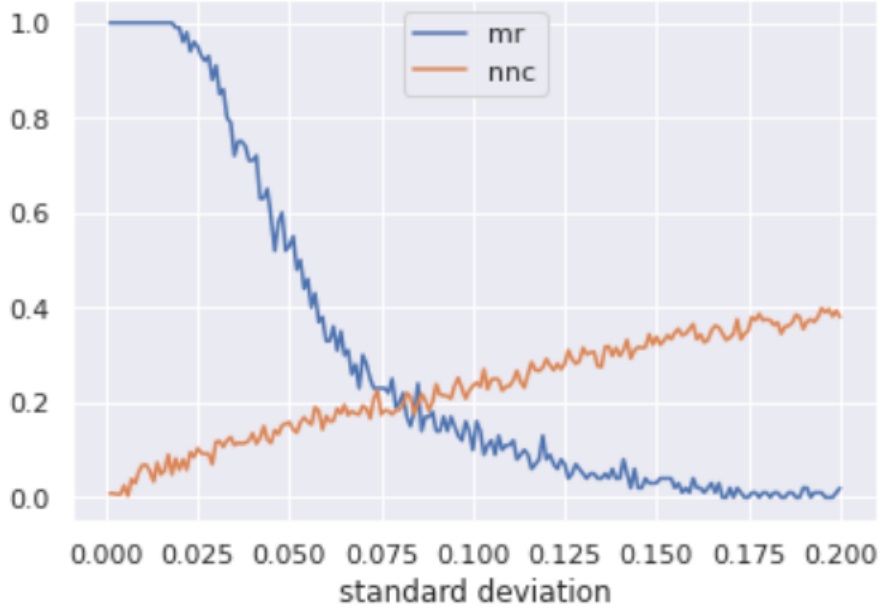


Figure 5.3: Development of  $nnc$  and  $mr$  for a dummy model with varying standard deviation  $\sigma$

For low values of  $\sigma$  (up to  $\sigma = 0.018$ ), all data points are classified as being memorized, i.e.  $mr = 1$ . With an increasing standard deviation, the memorizing ratio decreases until it reaches 0 at  $\sigma = 0.168$  and stays near the zero line. The  $nnc$  starts with its optimal value of 0 which means that both samples stem from the same distribution and then increases significantly indicating a progressively worse fit up to  $nnc = 0.4$ .

When we now compare this dummy model with our GAN-based model, we can state that the GAN-based model has a memorizing ratio of at most 0.1. At this point, we see a very low  $nnc$ -value of 0.02. This is much better than the dummy model where a memorizing ratio of 0.1 corresponds with a  $nnc$ -value of 0.235 which means that the two samples are recognized as being further apart than in the GAN-model even if the same number of points has been detected memorized. A  $nnc$ -value of 0.02 for the dummy model is only reached in configurations where all empirical points are detected as being memorized.

Next, we compare different GAN configurations and the behavior of the two measures in these different configurations. We analyze the behaviour for ten trained GANs differing in the number of layers in both networks. For the sake of readability, we here show the behavior of the  $nnc$  measure for only four of these GANs in Figure 5.4. Other configurations exhibit similar behavior. The abbreviation  $nnc(x, y)$  hereby refers to a GAN with  $x$  layers in the discriminator and  $y$  layers in the generator.

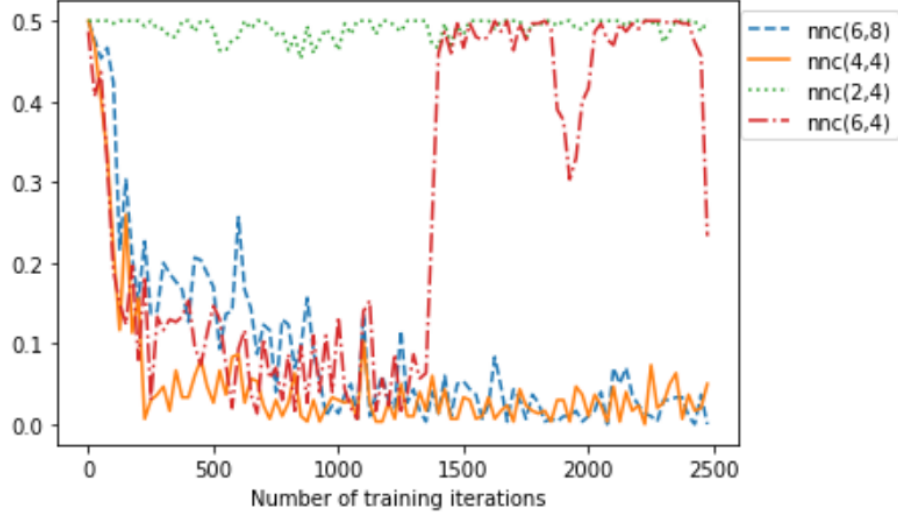


Figure 5.4: Development of the  $nnc$  for various GAN configurations

In Figure 5.4, one can see that the nearest neighbor coincidence in some configurations does not decrease but either stays near 0.5 (e.g.,  $nnc(2,4)$ ) or first decreases, but after some iterations sharply increases again (e.g.,  $nnc(6,4)$ ). A high and non-decreasing value of the  $nnc$  means that the GAN does not manage to learn the distribution of the empirical data. Therefore, these two configurations are not suitable. The other two configurations, however, lead to decreasing and low  $nnc$ -values with more training iterations. So, here, the GAN does learn to reproduce the empirical distribution and these two configurations seem appropriate. One can see in this example that the nearest neighbor coincidence measure is able to distinguish between configurations in which the generated data has the same distributions as the empirical data and configurations in which this is not the case. This approach can therefore be used to determine the optimal GAN configuration and to show in validation that the GAN reaches its target.

The development of the memorizing ratio also differs between those configurations differing in the number of layers in the discriminator and the generator, as Figure 5.5 shows.

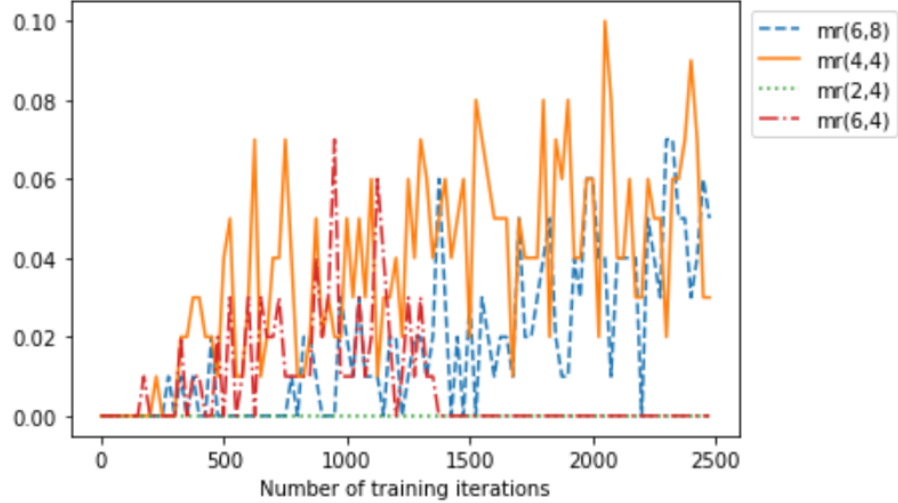


Figure 5.5: Development of the  $mr$  for various GAN configurations

In the non-converging configuration (see  $nnc(2,4)$  in Figure 5.4 above), the associated memorizing ratio  $mr(2,4)$  stays at 0. This can be interpreted that if the GAN does not replicate the underlying distribution, then it also does not remember the empirical data points either. For the configuration

(6, 4) with six layers in the discriminator and four layers in the generator, we see in Figure 5.4 that at first  $nnc$  decreases, but at iteration 1400 it sharply increases. The adverse behaviour between  $nnc$  and  $mr$  can be seen in this case: The  $mr(6, 4)$  increases at the beginning, but after iteration 1400 it decreases to 0. In this case, the GAN does not remember the empirical data points, but does not match the empirical distribution either. This configuration is also not desirable. For the two converging configurations (see  $nnc(4, 4)$  and  $nnc(6, 8)$  above), the memorizing ratio increases and rises up to 10%. This is as expected: in a configuration in which the GAN as instructed reproduces the empirical distribution, the memory effect also increases. For validation purposes, it makes sense to be aware of how many of the scenarios are memorized and to optimize the GAN configuration and training iteration such that both, the  $nnc$  and the  $mr$ , are low.

## 6 Conclusions

When using a machine learning based model for regulatory purposes, e.g. modelling of risks under Solvency 2, additional validation techniques have to be applied to take into account the specificities of these models. For validation purposes, as well as for the optimization of a machine learning risk model, we provided two specialized measures that can be used to evaluate the performance of the scenario generation: nearest neighbor coincidences (measuring the alignment of the dependencies between the risk factors) and a new measure, the memorizing ratio (measuring overfitting). We show that the memorizing ratio is able to detect the memorizing effect in GANs and that it has desired mathematical properties, i.e. it converges when the amount of data increases. Finally, using the example of a GAN-based ESG, we show how these measures behave during training iterations and how they can be used for validation and model selection.

## Acknowledgments and funding

S. Flaig would like to thank Deutsche Rückversicherung AG for the funding of this research. Opinions, errors and omissions are solely those of the authors and do not represent those of Deutsche Rückversicherung AG or its affiliates.

## Disclosure statement.

The authors report there are no competing interests to declare.

## References

- Sanjeev Arora, Andrej Risteski, and Yi Zhang. Do gans learn the distribution? some theory and empirics. In *International Conference on Learning Representations*, 2018.
- BaFin. Machine learning in risk models: Characteristics and supervisory priorities, 2021. URL <https://www.bundesbank.de/resource/blob/793670/61532e24c3298d8b24d4d15a34f503a8/mL/2021-07-15-ml-konsultationspapier-data.pdf>. [accessed on 2023/10/20].
- Ching-Yuan Bai, Hsuan-Tien Lin, Colin Raffel, and Wendy Chi-wen Kan. On training sample memorization: Lessons from benchmarking generative modeling with a large-scale competition. In *Proceedings of the 27th ACM SIGKDD Conference on Knowledge Discovery & Data Mining*, pages 2534–2542, 2021.
- Christoph Bennemann. *Handbuch Solvency II: von der Standardformel zum internen Modell, vom Governance-System zu den MaRisk VA*. Schäffer-Poeschel, Stuttgart, 2011.
- Peter J Bickel and Leo Breiman. Sums of functions of nearest neighbor distances, moment bounds, limit theorems and a goodness of fit test. *The Annals of Probability*, pages 185–214, 1983.
- Ali Borji. Pros and cons of gan evaluation measures. *Computer Vision and Image Understanding*, 179: 41–65, 2019.

- Paolo Cadoni. *Internal models and Solvency II*. Risk Books, London, 2014.
- Yize Chen, Pan Li, and Baosen Zhang. Bayesian renewables scenario generation via deep generative networks. In *2018 52nd Annual Conference on Information Sciences and Systems (CISS)*, pages 1–6. IEEE, 2018.
- Francois Chollet. *Deep learning with Python*. Manning, 2018.
- Rama Cont, Mihai Cucuringu, Renyuan Xu, and Chao Zhang. Tail-gan: Nonparametric scenario generation for tail risk estimation. *arXiv preprint arXiv:2203.01664*, 2022.
- Laurent Dupont, Olivier Fliche, and Su Yang. Governance of artificial intelligence in finance, 2020. URL [https://acpr.banque-france.fr/sites/default/files/medias/documents/20200612\\_ai\\_governance\\_finance.pdf](https://acpr.banque-france.fr/sites/default/files/medias/documents/20200612_ai_governance_finance.pdf). [accessed on 2023/10/20].
- Bruno Ebner, Norbert Henze, and Joseph E Yukich. Multivariate goodness-of-fit on flat and curved spaces via nearest neighbor distances. *Journal of Multivariate Analysis*, 165:231–242, 2018.
- European Union. Directive 2009/136/EC of the European parliament and of the council. *Official Journal of the European Union*, 337:11, 2009.
- Lucio Fernandez-Arjona. A neural network model for solvency calculations in life insurance. *Annals of Actuarial Science*, 15(2):259–275, 2021.
- Lucas Benedikt Fiechtner. Risk management with generative adversarial networks, 2019. URL [https://www.researchgate.net/publication/347440941\\_Risk\\_Management\\_with\\_Generative\\_Adversarial\\_Networks](https://www.researchgate.net/publication/347440941_Risk_Management_with_Generative_Adversarial_Networks). [accessed on 2023/10/20].
- Solveig Flaig and Gero Junike. Scenario generation for market risk models using generative neural networks. *Risks*, 10(11):199, 2022.
- Antoine Geller and Donatien Hainaut. Long short-term memory neural network for econometric forecasting: A comparison between a statistical method and a neural network in the case of value at risk. 2021. URL <http://hdl.handle.net/2078.1/thesis:33210>.
- Ian Goodfellow. Nips 2016 tutorial: Generative adversarial networks. *arXiv preprint arXiv:1701.00160*, 2016.
- Ian Goodfellow, Jean Pouget-Abadie, Mehdi Mirza, Bing Xu, David Warde-Farley, Sherjil Ozair, Aaron Courville, and Yoshua Bengio. Generative adversarial nets. *Advances in neural information processing systems*, 2014.
- Norbert Henze. A multivariate two-sample test based on the number of nearest neighbor type coincidences. *The Annals of Statistics*, 16(2):772–783, 1988.
- Th. Herrmann and B. Amendinger. Validierung eines Marktrisikomodells. In Marcus R. W. Martin, Peter Quell, and Carsten S. Wehn, editors, *Modellrisiko und Validierung von Risikomodellen - Regulatorische Anforderungen, Verfahren, Methoden und Prozesse*. Bank-Verlag GmbH, 2nd edition, 2017.
- Carsten Jung, Henrike Mueller, Simone Pedemonte, Simone Plances, and Oliver Thew. Machine learning in uk financial services. *Bank of England and Financial Conduct Authority*, 2019. URL <https://www.bankofengland.co.uk/-/media/boe/files/report/2019/machine-learning-in-uk-financial-services.pdf>. [accessed on 2023/10/20].
- Jiha Kim and Hyunhee Park. Limited discriminator gan using explainable ai model for overfitting problem. *ICT Express*, 2022.
- Alexei Kondratyev and Christian Schwarz. The market generator. *Available at SSRN 3384948*, 2019.
- Casey Meehan, Kamalika Chaudhuri, and Sanjoy Dasgupta. A non-parametric test to detect data-copying in generative models. In *International Conference on Artificial Intelligence and Statistics*, 2020.

- Pronoy K Mondal, Munmun Biswas, and Anil K Ghosh. On high dimensional two-sample tests based on nearest neighbors. *Journal of Multivariate Analysis*, 141:168–178, 2015.
- Vaishnavh Nagarajan, Colin Raffel, and Ian J Goodfellow. Theoretical insights into memorization in gans. In *Neural Information Processing Systems Workshop*, volume 1, 2018.
- Hao Ni, Lukasz Szpruch, Magnus Wiese, Shujian Liao, and Baoren Xiao. Conditional sig-wasserstein gans for time series generation. *arXiv preprint arXiv:2006.05421*, 2020.
- Dietmar Pfeifer and Olena Ragulina. Generating VaR scenarios under Solvency II with product beta distributions. *Risks*, 6(4):122, 2018.
- Eitan Richardson and Yair Weiss. On gans and gmms. *Advances in Neural Information Processing Systems*, 31, 2018.
- Mark F Schilling. Multivariate two-sample tests based on nearest neighbors. *Journal of the American Statistical Association*, 81(395):799–806, 1986.
- David Tobjörk. Value at risk estimation with generative adversarial networks. 2021.
- Joost van der Burgt. General principles for the use of artificial intelligence in the financial sector, 2019. URL <https://www.dnb.nl/media/voffsrc/general-principles-for-the-use-of-artificial-intelligence-in-the-financial-sector.pdf>. [accessed on 2023/10/20].
- Ryan Webster, Julien Rabin, Loic Simon, and Frédéric Jurie. Detecting overfitting of deep generative networks via latent recovery. In *Proceedings of the IEEE/CVF Conference on Computer Vision and Pattern Recognition*, pages 11273–11282, 2019.
- Lionel Weiss. Two-sample tests for multivariate distributions. *The Annals of Mathematical Statistics*, 31(1):159–164, 1960.
- Magnus Wiese, Lianjun Bai, Ben Wood, and Hans Buehler. Deep hedging: learning to simulate equity option markets. In *33rd Conference on Neural Information Processing Systems (NeurIPS 2019), Vancouver, Canada*, 2019.
- Magnus Wiese, Robert Knobloch, Ralf Korn, and Peter Kretschmer. Quant gans: Deep generation of financial time series. *Quantitative Finance*, 20(9):1419–1440, 2020.
- Qiantong Xu, Gao Huang, Yang Yuan, Chuan Guo, Yu Sun, Felix Wu, and Kilian Weinberger. An empirical study on evaluation metrics of generative adversarial networks. *arXiv preprint arXiv:1806.07755*, 2018.

## List of Tables

1	Expectation of the memorizing ratio for $n = 100$ simulations, with $m = 500$ (first number) and $m = 5000$ (second number) and different values of $\rho$ for the following distributions: standard normal, exponential with mean 1, t-distribution with with 1 degree of freedom, Cauchy with scale and location equal to 1, Pareto with scale and shape equal to 1. . . . .	9
---	--	---

## List of Figures

3.1	Neural network structure, based on Fernandez-Arjona (2021, Fig. 1) . . . . .	4
3.2	Neural network structure, in accordance with Chollet (2018, Chapter 8.5) . . . . .	5
4.1	Example for the benefit of the memorizing ratio; on the left: $nnc_{3,12} = 0$ , $mr_{0.5,12} = 0$ ; on the right: $nnc_{3,12} = 0$ , $mr_{0.5,12} = 0.5$ . . . . .	8
5.1	Development of the chosen validation measures $nnc$ and $mr$ for the GAN-based ESG . .	10

5.2	Comparison of two histograms for the distances between a generated point and its nearest empirical data point; left: 650 training iterations, $mr = 1\%$ ; right: 1300 training iterations, $mr = 8\%$	10
5.3	Development of $nnc$ and $mr$ for a dummy model with varying standard deviation $\sigma$	11
5.4	Development of the $nnc$ for various GAN configurations	12
5.5	Development of the $mr$ for various GAN configurations	12

# Appendix

## A Appendix: Proof of Theorem 6

We cite the following useful result:

**Theorem 7.** (Weiss, 1960). Let  $E_1, \dots, E_m, G_1, \dots, G_m$  be independent and identically distributed  $d$ -variate random variables. Assume  $E_1$  has a piecewise continuous and bounded probability density function  $f$ . Let  $\rho \in (0, 1]$  and

$$R_i := \rho \min_{i \neq j} |E_i - E_j|, \quad i = 1, \dots, m$$

and let  $S_i$  be the number of points  $G_1, \dots, G_m$  contained in the open sphere  $\{x : |x - E_i| < R_i\}$  for  $i = 1, \dots, m$ . Then the joint distribution of  $S_i$ ,  $S_i$  is the same as the joint distribution of  $S_{i'}$  and  $S_{i'}$  for any  $i \neq j$  and  $i' \neq j'$ . It further holds that

$$\lim_{m \rightarrow \infty} P[S_1 = s] = Q(s) := \int_{\mathbb{R}^d} \frac{\rho^{-d} f^{2+s}(x)}{(f(x) + \rho^{-d} f(x))^{s+1}} dx, \quad s \in \mathbb{N}_0 \quad (\text{A.1})$$

and

$$\lim_{m \rightarrow \infty} P[S_1 = s_1 \cap S_2 = s_2] = Q(s_1)Q(s_2), \quad s_1, s_2 \in \mathbb{N}_0.$$

*Proof.* Lionel Weiss proved the Theorem for  $\rho = \frac{1}{2}$  in Weiss (1960), but his proof works exactly the same for any  $\rho \in (0, 1]$ .  $\square$

Now, we can proof Theorem 6:

*Proof.* The proof is based on Theorem 7. It holds that

$$\begin{aligned} Q(0) &= \int_{\mathbb{R}^d} \frac{\rho^{-d} f^2(x)}{f(x) + \rho^{-d} f(x)} dx \\ &= \frac{1}{\rho^d + 1} \int_{\mathbb{R}^d} f(x) dx = \frac{1}{\rho^d + 1} < \infty. \end{aligned}$$

Let

$$R_i := \rho \min_{i \neq j} |E_i - E_j| = \rho R_{E_i}^1, \quad i = 1, 2, \dots, m$$

and

$$Z_i := \mathbf{1}_{[0, \rho R_{E_i}^1)} \left( \min_{j=1, \dots, m} |G_j - E_i| \right), \quad i = 1, 2, \dots, m.$$

Then  $mr_{\rho, m} = \frac{1}{m} \sum_{i=1}^m Z_i$ . It holds by Theorem 7 that

$$\begin{aligned} \mathbf{E}[Z_i] &= P \left[ \min_{j=1, \dots, m} |G_j - E_i| < \rho R_{E_i}^1 \right] \\ &= 1 - P \left[ \forall j : |G_j - E_i| \geq R_i \right] \\ &= 1 - P[S_i = 0] \\ &= 1 - P[S_1 = 0] \\ &\rightarrow 1 - Q(0) = \frac{\rho^d}{\rho^d + 1}, \quad i = 1, 2, \dots, \quad m \rightarrow \infty. \end{aligned} \quad (\text{A.2})$$



As  $Z_i^2 = Z_i$ , it follows that

$$\lim_{m \rightarrow \infty} \text{Var}(Z_i) = 1 - Q(0) - (1 - Q(0))^2 = Q(0) - Q^2(0) < \infty, \quad i = 1, 2, \dots$$

Let  $i \neq l$ . Then

$$\begin{aligned} \text{Cov}(Z_i, Z_l) &= \mathbf{E}[Z_i Z_l] - \mathbf{E}[Z_i] \mathbf{E}[Z_l] \\ &= P\left(\min_{j=1, \dots, m} |G_j - E_i| < \rho R_{E_i}^1 \cap \min_{j=1, \dots, m} |G_j - E_l| < \rho R_{E_i}^1\right) - (\mathbf{E}[Z_1])^2 \\ &= 1 - P[S_i = 0 \cup S_l = 0] - (E[Z_1])^2 \\ &= 1 - P[S_1 = 0 \cup S_2 = 0] - (E[Z_1])^2 \\ &= 1 - P[S_1 = 0] - P[S_2 = 0] + P[S_1 = 0 \cap S_2 = 0] - (\mathbf{E}[Z_1])^2 \\ &\rightarrow 1 - Q(0) - Q(0) + Q^2(0) - (1 - Q(0))^2 = 0, \quad m \rightarrow \infty. \end{aligned}$$

Hence, by Bienaymé's identity

$$\begin{aligned} \mathbf{E}\left[|mr_{\rho, m} - E[Z_1]|^2\right] &= \text{Var}\left(\frac{1}{m} \sum_{i=1}^m Z_i\right) \\ &= \frac{1}{m^2} \left( \sum_{i=1}^m \text{Var}(Z_i) + \sum_{i \neq l} \text{Cov}(Z_i, Z_l) \right) \\ &= \frac{1}{m^2} (m \text{Var}(Z_1) + (m^2 - m) \text{Cov}(Z_1, Z_2)) \rightarrow 0, \quad m \rightarrow \infty. \end{aligned}$$

Further, by the Minkowski inequality and Equation (A.2), it holds that

$$\begin{aligned} &\sqrt{\mathbf{E}\left[\left|mr_{\rho, m} - \frac{\rho^d}{\rho^d + 1}\right|^2\right]} \\ &\leq \sqrt{\mathbf{E}\left[|mr_{\rho, m} - E[Z_1]|^2\right]} + \sqrt{\mathbf{E}\left[\left|E[Z_1] - \frac{\rho^d}{\rho^d + 1}\right|^2\right]} \rightarrow 0, \quad m \rightarrow \infty. \end{aligned}$$

□